

Reflective correctors for the Hubble Space Telescope axial instruments

Murk Bottema

Reflective correctors to compensate the spherical aberration in the Hubble Space Telescope are placed in front of three of the axial scientific instruments (a camera and two spectrographs) during the first scheduled refurbishment mission. The five correctors required are deployed from a new module that replaces the fourth axial instrument. Each corrector consists of a field mirror and an aspherical, aberration-correcting reimaging mirror. In the camera the angular resolution capability is restored, be it in reduced fields, and in the spectrographs the potential for observations in crowded areas is regained along with effective light collection at the slits.

Introduction

When the spherical aberration in the Hubble Space Telescope (HST) was discovered, two second-generation axial instruments were in advanced stages of design at the Ball Electro-Optics and Cryogenics Division (BECD), namely, the Near-Infrared Camera and Multiple-Object Spectrograph (NICMOS) and the Space Telescope Imaging Spectrograph (STIS). Our first concern was to find a means to correct the spherical aberration in these two instruments. In NICMOS this was quite simple. The optical train starts with a two-mirror relay consisting of a reimaging mirror and a beam-steering mirror. The latter directs the telescope image to the various NICMOS cameras and spectrographs and is placed at a conjugate of the telescope primary mirror, which is the source of the spherical aberration. Correction required nothing more than aspherization of the beam-steering mirror. No changes in the optical configuration were necessary. STIS is a multimode spectrograph in which originally a slit wheel was placed directly at the telescope image plane. To remove the spherical aberration before the light enters the slits, we have to move the slit wheel back and place a two-mirror corrector in front of it. Again

the second mirror is an asphere at a conjugate of the telescope primary mirror.

In July 1990 the NASA Goddard Space Flight Center asked us also to investigate a means of correction for the Goddard High Resolution Spectrograph (GHRS), already on orbit. After exploring various refractive and reflective solutions, we also suggested here a two-mirror corrector but left the question open of how such a corrector could be installed on orbit.

In August 1990 the Space Telescope Science Institute formed a panel (the HST strategy panel) to assess a means of recovering the scientific potential of the HST. With regard to the axial instruments the panel adopted the GHRS corrector concept and recommended that it be applied to the faint-object camera (FOC) and the faint-object spectrograph (FOS) as well. The fourth instrument, the high-speed photometer, was to be replaced by a new module, the Corrective Optics Space Telescope Axial Replacement (COSTAR), to form a basis for deployment of the corrector systems.¹ The COSTAR idea was proposed by Crocker and fits naturally in the HST program for on-orbit instrument replacement.² COSTAR is to be installed during the first scheduled refurbishment mission, now planned for late 1993. In the same mission the fifth instrument, the Wide Field and Planetary Camera (WF/PC), will be replaced by a new version (WF/PC II). Its optics are modified to compensate the spherical aberration internally. STIS and NICMOS, the original early-replacement candidates, are now rescheduled for possible later refurbishment missions.

The author was a consultant to the Ball Electro-Optics and Cryogenics Division, P.O. Box 1062, Boulder, Colorado 80306-1062. He is now deceased.

Received 13 April 1992.

0003-6935/93/101768-07\$05.00/0.

© 1993 Optical Society of America.

Corrector Principle

The primary mirror of the telescope was intended to have a conic constant

$$CC1 = -1.0023 \quad (\text{design}).$$

The actual conic constant was derived from records of the mirror fabrication and also from an analysis of the FOC and WF/PC images. The generally accepted value is

$$CC1 = -1.0139 \quad (\text{actual}),$$

with a one-sigma uncertainty $\sigma CC = 0.0002$. The mirror is flatter than intended with an edge deviation $z_1 = -2.2 \mu\text{m}$. The associated spherical aberration in the telescope has a diameter of 0.43 mm (1.54 arcsec) at the circle of least confusion. The telescope was specified to have diffraction-limited image quality at 633 nm, i.e., the angular resolution should have been ~ 0.05 arcsec, and the rms wave-front error at the focal point should not be larger than 0.071 waves at 633 nm. At the optimum focus setting the actual rms wave-front error is 0.41 waves at 633 nm.³

In COSTAR each corrector consists of a spherical field mirror M1 and an aspherical reimaging mirror M2 (Fig. 1). The function of M1 is to image the telescope primary mirror at M2. A spherical mirror suffices. M2 has three functions:

- (1) To image the telescope at the entrance port of the scientific instruments.
- (2) To compensate for the HST spherical aberration.
- (3) To restore the astigmatism in the corrector image to the value for which the scientific instrument was originally designed.

As indicated in Fig. 1, M2 is located on the original chief ray to the scientific instrument. M2 is a fourth-

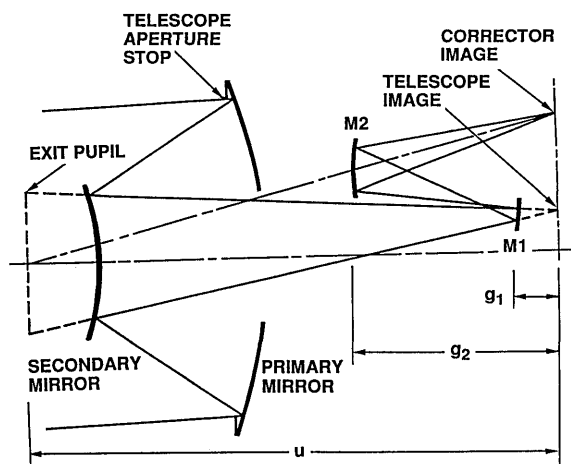


Fig. 1. Corrector principle. The field mirror M1 images the telescope primary mirror at M2. This mirror, an anamorphic fourth-order asphere, compensates the spherical aberration in the telescope.

order anamorphic asphere. The fourth-order term compensates for the spherical aberration and must be slightly anamorphic because the corrector mirrors do not form a centered system. Control of astigmatism requires M2 to be anamorphic of the second order also.

In total five sets of correctors are required. They serve the two cameras in the FOC ($f/48$ and $f/96$ cameras), the short-wavelength spectrograph in the FOS (FOS blue), the long-wavelength spectrograph in the FOS (FOS red), and the GHRS. The mirror sets for the two FOC cameras are identical, as are those for the two FOS spectrographs. Hence there are only three different classes of prescription by which the mirrors must be fabricated. The optical parameters are listed in Table 1. The five M2 mirrors have in common that the edge values of the fourth-order figure terms are in essence the same and opposite to the edge deviation z_1 in the primary mirror. The fabrication of such mirrors is not trivial but appears to be within the state of the art of advanced computer-controlled figuring techniques. The deviations from the prescribed profiles are expected to be smaller than 0.01 waves rms at 633 nm and when combined with a surface roughness, smaller than 1 nm rms.

COSTAR

The main structure of COSTAR is a thermally stable graphite-epoxy truss mounted in a standard orbital-replacement instrument enclosure. On orbit, a small optical bench, also made of graphite epoxy, is deployed through an aperture below the A latch (Fig. 2). Subsequently four arms are folded out and locked in position by overcenter springs. One arm carries the two M1 mirrors for the FOC and a second arm the two M2 mirrors. The third arm carries the two FOS M2 mirrors and the fourth arm the GHRS M2 mirror. The M1 mirrors for the FOS and GHRS are mounted directly on the deployable optical bench (Fig. 3).

The four arms are operated independently and do not interfere with each other's functions, when either deployed or stowed. All mechanisms have built-in redundancy. It is expected that COSTAR will be in operation for at least three years, i.e., until on or more of the axial instruments are replaced. In view of this the arms are hinged so that they fold back automatically when the optical bench is retracted.

Table 1. Mirror Parameters

Instrument	FOC	FOS	GHRS
M1 radius of curvature (mm)	613	586	801
M2 profile coefficients ^a			
D1 (10^{-3} mm^{-1})	1.710	1.661	1.174
D2	1.003	1.131	1.033
D3 (10^{-7} mm^{-3})	9.78	9.74	3.25
D4	1.005	1.235	1.040
Y diameter of primary-mirror image (mm)	13.8	14.0	18.4

^aM2 profile: $Z = D1(D2 X^2 + Y^2) + D3(D4 X^2 + Y^2)^2$.

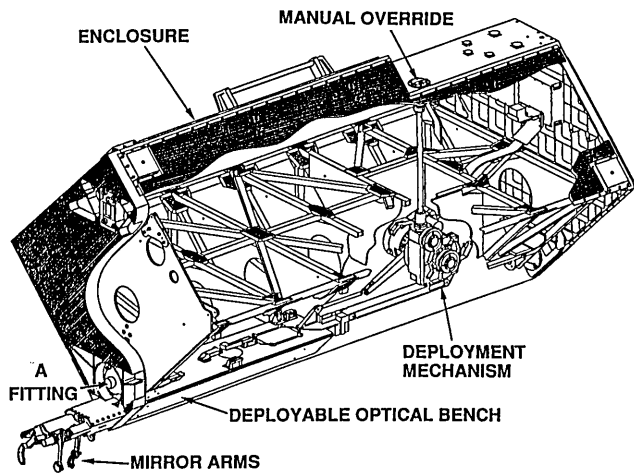


Fig. 2. COSTAR. Arms carrying the corrector mirrors are folded out on orbit from a deployable optical bench. The overall size of the enclosure is $88 \times 88 \times 220 \text{ cm}^3$.

In an emergency all mirrors can thus be removed simultaneously. COSTAR is then no longer operational. The optical bench is moved by a motor-driven crankshaft mechanism controlled from the ground. In an emergency the bench can be retracted manually by an astronaut in extravehicular activity. The manual override assures that COSTAR can be removed from the HST, even if all powered retraction fails.

Imaging Properties

In general the telescope focal ratio ($f/24$) is not preserved by the corrector system. If M1 is placed in front of the telescope focal plane, as shown in Fig. 1, an intermediate field image is formed between M1 and M2. This image is magnified by M2, leading to a corrector focal ratio that is larger than $f/24$. In the paraxial approximation the internal magnification is

$$M_c = (1 - g_1/u)/(1 - g_1/g_2), \quad (1)$$

where g_1 , g_2 , and u are the distances of M1, M2 and the telescope exit pupil, respectively, from the tele-

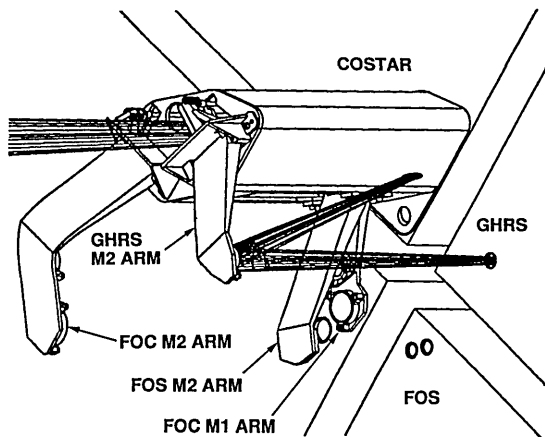


Fig. 3. Mirror arms and light path of the GHRS corrector.

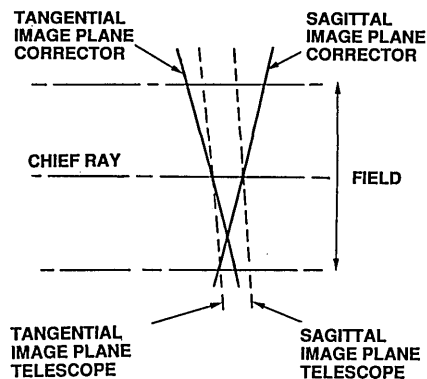


Fig. 4. Image-plane tilts in the corrector field.

scope focal plane (Fig. 1). Evidently $M_c = 1$ only if $g_1 = 0$.

The two-mirror corrector permits control of astigmatism in a single field point only. This point is defined by the chief ray. The field around this point is astigmatic as a result of the difference in tilt between the tangential and sagittal image planes (Fig. 4). The difference is approximately equal to the deviation angle of the chief ray at M2. There is only a mirror contribution from M1. In general the tangential and sagittal image planes do not conform to those of the telescope either in tilt or in curvature. The result is an asymmetrically distributed astigmatism in the field of the scientific instrument.

Because M2 is placed at a conjugate of the telescope primary mirror, the field is in principle free of coma. However, separate tangential and sagittal mirror images are formed by M1. Precisely as the field images are, they are tilted differently and also axially separated. Thus, as a second-order effect, some coma still appears in the corrector field.

FOC Correctors

The configuration of the FOC correctors was driven by the requirement that the effects of the tangential and sagittal image-plane tilts be kept as small as possible. To achieve this M1 had to be placed in front of the FOC enclosure (Fig. 5). The M1 distance g_1 was constrained further by the presence of thermal-isolation blankets between the scientific instruments. These protrude into the area in front of the scientific instruments but how far is not known well. The M1 arm must clear the blankets by an adequate margin. A distance $g_1 = 210 \text{ mm}$ was considered to be a safe

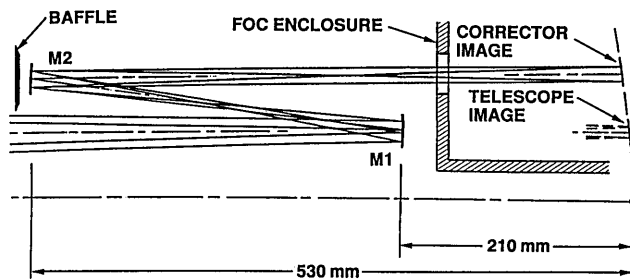


Fig. 5. Schematic of the FOC corrector.

minimum. The distance of M2 from the telescope focal plane was limited by the condition that light scattered by the M2 arm cannot enter the wide-field/planetary camera (WF/PC) directly. This led to $g_2 = 530$ mm. The paraxial corrector magnification then is $M_c = 1.61$. This results in nominal corrector focal ratios of $f/77$ and $f/154$ for the $f/48$ and $f/96$ cameras, respectively.

The FOC optics were designed originally for a telescope exit-pupil distance of ~ 7 m. In the correctors the pupil distance is 530 mm. Consequently the angle, subtended by the camera field at the pupil, becomes an order of magnitude larger. In the $f/77$ camera this causes severe vignetting. Its field covers a 28-arcsec-square acquisition field (44 arcsec square at $f/48$) as well as a 13-arcsec slit (20 arcsec at $f/48$) for spectral imaging. To make the best of the situation the chief ray is placed at the intersection P of the acquisition field and the slit (Fig. 6). The scientific observations are done in a subfield, which is 14 arcsec square and can be positioned anywhere in the acquisition field. The subfield is now placed adjacent to P. Most of this field and approximately one fifth of the slit then remain unvignetted.

In the $f/154$ camera the acquisition field is 14 arcsec square, and the chief ray is placed at its center. All but the extreme corners of the field then remain unvignetted.

To illustrate the achievable image quality in the $f/77$ camera we present here geometrical-optical aberrations in the imaging subfield and the spectrograph slit (Fig. 7). They were derived from an optical model that included the aberrated Optical Telescope Assembly (OTA), the corrector, and the $f/48$ camera optics. Perfect mirror figures and perfect alignment are assumed. At P the image is virtually stigmatic. Across the field and along the slit the aberrations increase to a full diameter of ~ 0.1 arcsec. This suggests that the originally expected angular resolution capability of ~ 0.05 arcsec can be restored closely only in the immediate vicinity of P. We recall that with a perfect telescope the aberrations

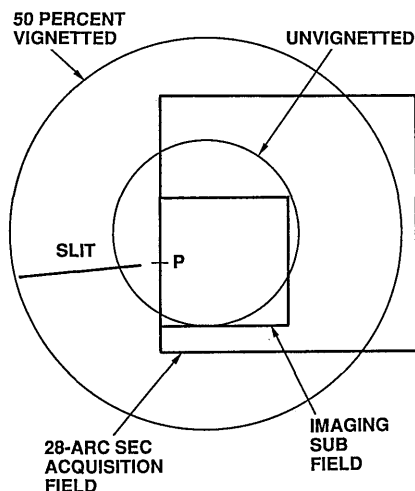


Fig. 6. Vignetting in the field of the FOC $f/77$ camera.

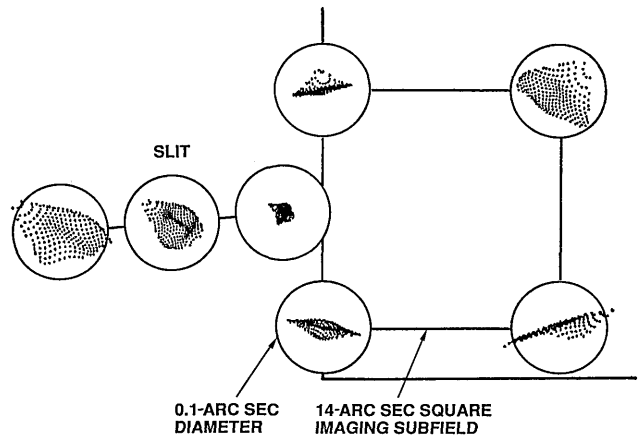


Fig. 7. Aberrations in the imaging subfield and along the spectrograph slit of FOC $f/77$ camera, as seen projected back on the sky.

in the $f/48$ camera would be smaller than one detector pixel (0.043 arcsec square) in the entire acquisition field. Although the $f/77$ camera compensates the spherical aberration effectively, it clearly cannot match this performance.

At $f/77$ the width of the spectrograph slit is only 0.06 arcsec (0.10 arcsec at $f/48$). In addition to vignetting there is also light loss from partial sampling of the telescope image. No effort is made here to analyze this quantitatively.

The acquisition field of the $f/154$ camera is of the same size as the imaging subfield in the $f/77$ camera. The aberrations are of comparable size, as shown in Fig. 8. Obviously the $f/154$ imaging subfield (7 arcsec square) should be positioned preferably near the center of the acquisition field.

FOS Correctors

The two FOS spectrographs, FOS blue and FOS red, are placed side by side in the FOS enclosure. The center-to-center distance between their entrance ports is 16 mm. To keep the beams at the M2 mirrors well

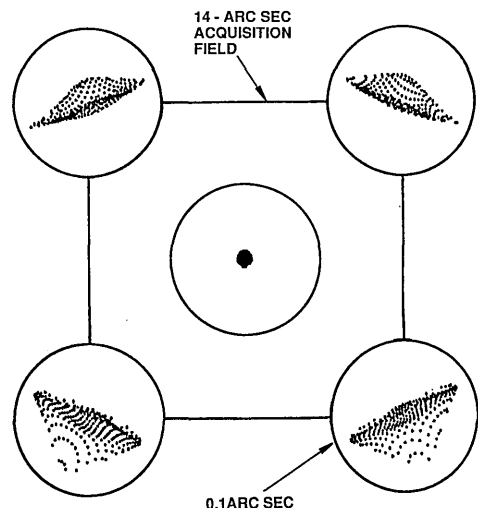


Fig. 8. Aberrations in the acquisition field of the FOC $f/154$ camera.

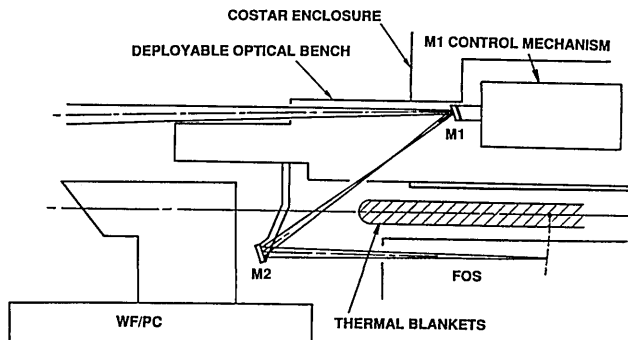


Fig. 9. Schematic of the FOS corrector.

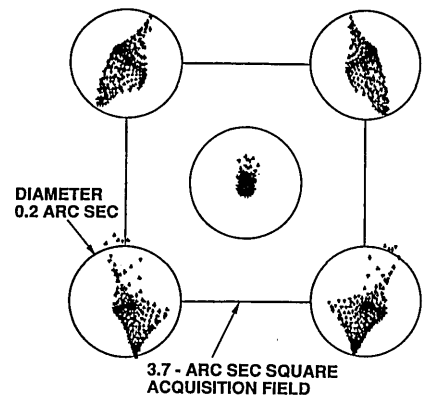


Fig. 10. Aberrations in the field of the FOS blue corrector.

separated, it was necessary to limit the distance of the M2's from the OTA focal plane to $g_2 = 365$ mm (Fig. 8). A second constraint, i.e., clearance between the M2 arm and the WF/PC pick-off mirror assembly, is also met at this distance.

The field mirrors M1 are mounted directly on the deployable optical bench. The distance from the telescope focal plane was set to $g_1 = 125$ mm. This results in a corrector focal ratio near $f/28$. This focal ratio permits a small but adequate margin for alignment errors between the corrector output beam and the $f/24$ spectrograph optics. As is evident from Fig. 8 the deviation angles at M1 and M2 are rather large (~ 39 deg), which causes large tilt differences between the tangential and sagittal image planes. This is acceptable since the largest slits, which define the acquisition field of the FOS, are only 3.6 arcsec square at $f/28$ (4.3 arcsec square at $f/24$).

The large deviation angles in the FOS correctors cause an anisotropy in the focal ratio. The paraxial approximation in Eq. (1) is not valid. The exact focal ratios were derived from optical modeling and are $f/27.6$ in the meridional plane of the corrector and $f/28.5$ orthogonal to this plane. The associated anisotropy in the plate scale must be taken into account in the FOS acquisition procedures and also in image processing. In the arrangement in Fig. 9 a generous margin is left for clearance between the light beams from M1 to M2 and the thermal insulation blankets between the FOS and COSTAR.

The original FOS optics were designed without the compensation of telescope astigmatism. The slits were placed in the telescope image surface of mean curvature at a distance of 60 mm from the telescope axis. The correctors are designed to produce stigmatic images at these slits. The correctors cover an acquisition field of 3.7 arcsec (4.3 arcsec at $f/24$). The aberrations in this field are shown in Fig. 10. From a nearly stigmatic center the aberrations increase to ~ 0.2 arcsec, full diameter, at the corners of the field. In single-object spectroscopic observations round slits are used at the center of the field. These range in diameter from 0.3 to 0.9 arcsec (1.0 arcsec at $f/24$). For these slits the intended image quality is fully restored. The FOS also has observational modes in which object and sky comparisons are made by means of slit pairs at opposite distances of 1.3 arcsec

from the center. The most commonly used slits are 0.21 arcsec square (0.25 arcsec at $f/24$) or larger. Here too the image quality is adequate. Also available are slit pairs, 0.1 arcsec square. Only for these is the image quality markedly compromised.

GHRS Corrector

The GHRS has two fixed slits at 90 mm from the OTA axis. Each of these is formed by separate tangential and sagittal slit pairs with an axial separation of 1.2 mm (Fig. 11). The smaller slit is placed on the chief ray. The telescope astigmatism is compensated in the GHRS optics. The two slits are served by a single corrector. The field mirror M1 is again mounted directly on the deployable optical bench with $g_1 = 100$ mm. The distance of M2 is $g_2 = 500$ mm. The focal ratio is $f/27.4$ with only 0.1% anisotropy. The light path is shown in Fig. 3. In the small slit (0.22 arcsec square at $f/27.4$, 0.25 arcsec square at $f/24$) the corrector images consist of narrow tangential and sagittal lines that are parallel to the

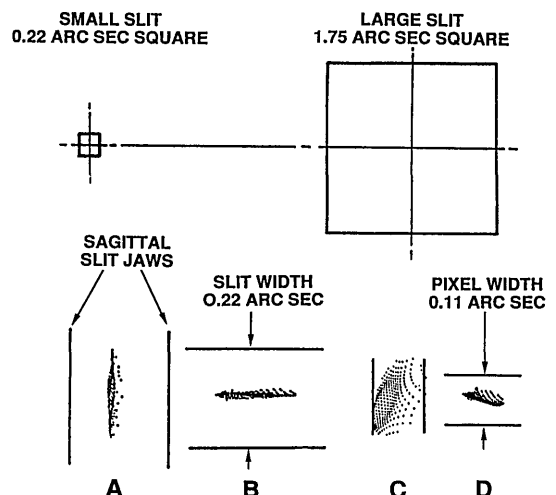


Fig. 11. Aberrations in the field of the GHRS corrector. A and B represent the sagittal and tangential corrector images, respectively, in relation to the sagittal and tangential slit jaws that form the small slit. C and D represent the sagittal and tangential images, respectively, at the center of the large slit in relation to the detector pixel size.

slit jaws. Hence excellent restoration of image quality is achieved. The larger slit, at 3.3 arcsec from the small slit, is used primarily for acquisition and imaging and is 1.75 arcsec square (2.0 arcsec at $f/24$). The slit area is scanned by 0.23-arcsec-square detector pixels. The aberrations in the large slit are of the same magnitude. Here too the restoration of image quality is satisfactory.

On-Orbit Focus Control

For all orbital-replacement instruments NASA has stipulated an on-orbit focus adjustment range $\Delta F = \pm 3$ mm. Of prime concern is focus control in the FOC. The device used here is the deployable optical bench. With the crankshaft mechanism operating at the end of its range, focus control to better than 0.1 mm can be realized easily. To be sure the two cameras have internal focus controls, but they are primarily intended for compensation of filter thicknesses and cannot cover the stipulated range. The advantage of using the deployable optical bench is that pupil imaging, i.e., imaging of the primary mirror at M2, is not noticeably affected. For small bench displacements the relative variation of the distance from the telescope exit pupil to M1 is insignificant and the distance between M1 and M2 remains constant.

The second function of focus control is to minimize the effects of residual spherical aberration that arise from a difference $\Delta CC1$ between the actual conic constant of the telescope primary mirror and the value assumed for the design of COSTAR. If any spherical aberration is detected by analysis of the FOC images, the focus can be reset for the point where the associated rms wave-front error is at a minimum. With $\Delta CC1 = 0.0005$, for example, the image quality would then not degrade by more than 0.023 waves rms at 633 nm. This is $\sim 10\%$ of the original HST rms wave-front error budget.

The mechanical adjustment range of the deployable optical bench is ± 8 mm. This permits coverage of the combinations of Δf and $\Delta CC1$, as shown in Table 2. The adjustment range was established early in the COSTAR program when the uncertainty in $CC1$ was much larger than that known at the present time and should be more than adequate to cover any contingencies.

In the spectrograph correctors, focus is controlled by the additional axial adjustment of M1 after the focus setting for the FOC is established. The corrective motion required is rather small. Since pupil imaging is not preserved, spherical aberration is induced, which combines with that from $\Delta CC1$. By

Table 2. Combinations of Focus Uncertainty Δf and Conic-Constant Uncertainty $\Delta CC1$ Covered by FOC Focus Mechanism

Δf (mm)	$\Delta CC1$
± 4.9	0
± 3.8	0.0005
± 2.6	0.0010

Table 3. Optimum Position of Field Mirror M1 and Associated Aberrations at the Small Slit in the GHRs Corrector for Some Combinations of the Focus Uncertainty Δf and the Conic-Constant Uncertainty $\Delta CC1$

Δf (mm)	$\Delta CC1$	M1 Position Regarding Bench (mm)	Aberration Diameter	
			Tangential (arcsec)	Sagittal (arcsec)
-3	0.005	-0.88	0.11	0.14
-3	0	-0.68	0.03	0.04
-3	-0.005	-0.48	0.14	0.11
3	0.0005	0.59	0.14	0.18
3	0	0.74	0.04	0.06
3	-0.0005	0.96	0.10	0.07

way of example we show in Table 3 the optimum M1 settings at the small slit in the GHRs corrector in case $\Delta f = \pm 3$ mm and $\Delta CC1 = \pm 0.0005$. The focus setting was selected to minimize the mean of the aberration diameters in the tangential and sagittal image planes. Evidently, even in these extreme cases, the throughput through the small slit and the angular resolution in the large slit will not be degraded seriously. A quantitative assessment must take into account diffraction, residual alignment errors, mirror imperfections, pointing jitter, and environmental effects. This is beyond the scope of this paper.

At the present time the paraxial focus of the telescope is placed 13 mm in front of the focal plane. We selected this position to maximize the flux through a 0.2-arcsec-diam field stop in the focal plane. The 0.25-arcsec spectrograph slits then collect $\sim 15\%$ of the light from the telescope. The current setting will be preserved when COSTAR is installed. It will permit occasional observations with retracted mirrors, although such observations are not planned regularly. In the GHRs this may be of advantage below 120 nm, where the transmission of the corrector drops sharply. In the FOS it preserves the potential for polarimetry, which is completely lost by polarization at the corrector mirrors.

Alignment

After deployment from COSTAR each corrector system must meet three alignment conditions:

- (1) M2 must be centered on the original chief ray to the scientific instrument (see Fig. 1).
- (2) The image of the telescope primary mirror must match M2.
- (3) The corrector image must be positioned at the entrance port of the scientific instrument.

The first condition can be met entirely by pre-launch alignment. As part of the COSTAR development the lateral positions of the entrance ports of the scientific instruments relative to the HST reference structure were derived from records of assembly and integration of the HST as well as from on-orbit mapping of the HST field. The remaining uncertainties are no larger than ~ 0.7 mm. In the FOC

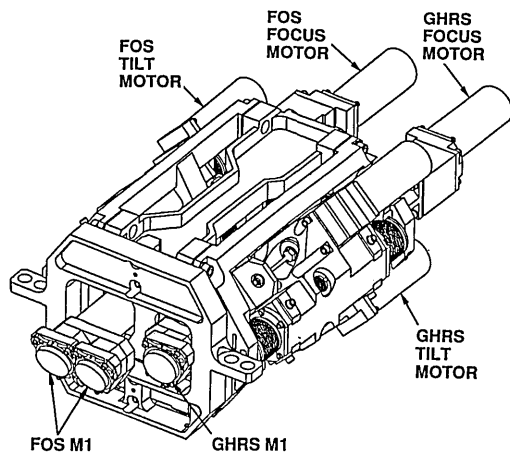


Fig. 12. Mechanism for on-orbit control of focus and alignment in the FOS and GHRS correctors. Only one of each pair of motors for control of the biaxial tilt is visible.

residual centering errors have no other effect than small shifts in the vignetted area (Fig. 6). In the GHRS corrector an alignment margin of 1.5 mm is available (which is the difference between $f/28$ and $f/24$ beams at $g_2 = 530$ nm) on top of a margin built into the GHRS optics. Even with the worst combination of lateral position errors between the GHRS and COSTAR, the small slit should remain unvignetted. Some vignetting may occur in the large slit but not by more than a few percent. In the FOS corrector the alignment margin is only 1.0 mm ($g_2 = 365$ nm), and the risk of some vignetting is correspondingly larger but still small.

The second alignment condition, centering of the primary-mirror image at M2, requires precise on-orbit control. This is done by biaxial tilt of M1 under command from the ground. Decentering errors cause field-independent coma. Centering to $\sim 1\%$ of the pupil-image diameter is necessary to keep the coma wave-front error to < 0.01 waves rms at 633 nm.⁴ The M1 mechanisms are designed to permit control to 0.004 waves rms or better. The presence of coma is monitored by image processing. The control accuracy probably exceeds the detection limit. The correction of coma includes other sources as well, such as decentering or tilt of the telescope secondary mirror.

The two FOC correctors share a single tilt and focus mechanism. The current plan is to use the $f/154$ camera for coma control on orbit and to depend on preflight coalignment of the two M1's for coma control in the $f/77$ camera. On-orbit adjustment is then not necessary when switching from one camera to the other. The same procedure is followed in the FOS. The on-orbit alignment will be done in FOS blue. The mechanism for focus and tilt control in the FOS and GHRS correctors is shown in Fig. 12.

The third alignment condition, centering of the corrector image, is a matter of telescope pointing and will be part of the COSTAR acquisition procedures.

Conclusions

COSTAR promises to compensate the spherical aberration in the HST within the limits set by the uncertainty in the conic constant of the primary mirror on one hand and the achievable figure quality of the corrector mirrors on the other. In the FOC the impact of correction is an increase in plate scale and some vignetting. Only in part of the scientific imaging fields can the image quality be restored fully to the intended levels. Some vignetting will also occur along the slit of the imaging spectrograph of the $f/48$ camera along with some loss of spatial resolution.

The $f/48$ camera was designed to include coronagraphic modes of observations. This capacity is lost because of the spherical aberration and will not be restored by COSTAR. The $f/96$ camera includes an $f/288$ superresolution mode. It is useless at the present time and will remain so with COSTAR. In spite of the above restrictions COSTAR will restore the potential for the quantitative radiometric measurements for which the FOC was intended. At the present time the radiometer fidelity is severely compromised by the spherical aberration.

In the spectrographs the removal of spherical aberration will restore the capability for observation of isolated objects in crowded fields and in addition improve the concentration of light in the small slits by a factor of 4 or more. Reflection losses in the COSTAR mirrors will reduce the efficiency of the scientific instruments but become significant only below 120 nm. The corrector throughput at this wavelength is expected to exceed 55% and to drop below 10% at 115 nm.

This work was done with the cooperation of the COSTAR team at Ball Electro-Optics and Cryogenics Division and was supported by contracts from the National Aeronautics and Space Administration.

References and Notes

1. R. A. Brown and H. C. Ford, eds., *A Strategy for Recovery* (Space Telescope Science Institute, Baltimore, Md., 1991), pp. 7-14.
2. J. H. Crocker, "Fixing the Hubble Space Telescope," in *Space Astronomical Telescopes and Instruments*, P. Y. Bély and J. B. Breckinridge, eds., Soc. Photo-Opt. Instrum. Eng. **1494**, 2-8 (1991).
3. The optimum focus lies at a fraction $(1 + \beta^2)/2$ of the distance from the paraxial focus to the marginal focus. Here β is the linear central obscuration ratio. In the HST $\beta = 0.33$.
4. In an unobscured system the relation between the rms wave-front error WFE , the pupil-image diameter d , the decentering h , and the primary-mirror edge deviation z_1 is

$$WFE = (2/3)\sqrt{2}(h/d)z_1.$$

With $h/d = 0.01$ and $z_1 = 2.23 \mu\text{m}$ we find $WFE = 0.0086$ waves rms at 633 nm.